# Optimal Operation of Power Systems With Energy Storage Under Uncertainty: A Scenario-Based Method With Strategic Sampling

Ren Hu<sup>©</sup>, Graduate Student Member, IEEE, and Qifeng Li<sup>©</sup>, Senior Member, IEEE

Abstract—The multi-period dynamics of energy storage (ES), intermittent renewable generation and uncontrollable power loads, make the optimization of power system operation (PSO) challenging. A multi-period optimal PSO under uncertainty is formulated using the chance-constrained optimization (CCO) modeling paradigm, where the constraints include the nonlinear energy storage and AC power flow models. Based on the emerging scenario optimization method which does not rely on pre-known probability distribution, this paper develops a novel solution method for this challenging CCO problem. The proposed method is computationally effective for mainly two reasons. First, the original AC power flow constraints are approximated by a set of learning-assisted quadratic convex inequalities based on a generalized least absolute shrinkage and selection operator (LASSSO). Second, considering the physical patterns of data and driven by the learning-based sampling, the strategic sampling method is developed to significantly reduce the required number of scenarios by different sampling strategies. The simulation results on IEEE standard systems indicate that 1) the proposed strategic sampling significantly improves the computational efficiency of the scenario-based approach for solving the chance-constrained optimal PSO problem, 2) the data-driven convex approximation of power flow can be promising alternatives of nonlinear and nonconvex AC power flow.

Index Terms—Chance-constrained, power flow, scenario optimization, LASSO, data-driven.

#### NOMENCLATURE

C .	7	7 7.
sets	ana	Indices

n	Number of buses (nodes) in the system
i, j	Index for the buses, $i, j = 1, 2,, n$ .
T'	Index set of the time periods.
t	Index for any time-period, $t \in T'$ .
S'	The scenario set.
S'	Length of the scenario set.
s, i', j'	Index for any scenario, $s, i', j' \in S'$ .

Manuscript received June 9, 2021; revised September 9, 2021 and October 28, 2021; accepted November 7, 2021. Date of publication November 15, 2021; date of current version February 21, 2022. This work was supported by the U.S. National Science Foundation under Award 2124849. Paper no. TSG-00900-2021. (Corresponding author: Qifeng Li.)

The authors are with the Department of Electrical and Computer Engineering, University of Central Florida, Orlando, FL 32816 USA (e-mail: hurenlakerr@knights.ucf.edu; qifeng.li@ucf.edu).

Color versions of one or more figures in this article are available at https://doi.org/10.1109/TSG.2021.3127922.

Digital Object Identifier 10.1109/TSG.2021.3127922

P	ar	an	ne	tei	rs

 $P_{i,t(frt)}^{net}$ 

$c_{i1}(c_{i2})$	Coefficients of the generator's genera-					
	tion cost.					
$G_{ij}(B_{ij})$	Real (imaginary) part of the line admittance.					
$r_i^{eq}(r_i^{cvt})$	Equivalent resistance of the battery					
	(converter).					
$V_{i,t}^{min}, V_{i,t}^{max}$	Lower and upper limits of bus voltage mag-					
.,,	nitude.					
$P_{i,t}^{gmin}, P_{i,t}^{gmax}$	Lower and upper limits of the generator's					
amin amay	active power.					
$Q_{i,t}^{gmin}, Q_{i,t}^{gmax}$	Lower and upper limits of the generator's					
	reactive power.					
$S_{ij,t}^{gmax}$	Maximum apparent power of power trans-					
J,-	mission.					
$E_{ES,i}^{min}, E_{ES,i}^{max}$	Capacity limits of energy storage.					
$E_{ES,i,0}$	Initial energy status of energy storage.					
$S_{ES,i}^{max}$	Maximum apparent power of energy storage.					
α	Probability level.					
$\epsilon$	Violation probability level.					
β	Confidence level.					
$\omega_{pi}(\omega_{qi})$	Participation factors of the generator's or					
	energy storage's active (reactive) power.					

Forecast values of the net reactive load

Forecast values of the net active load input of power loads and renewable energy gener-

inputs of PLREG.

ations (PLREG).

 $\Delta p_i^s$ ,  $\Delta q_i^s$ Corresponding forecast errors of the net active and reactive power inputs.

 $C^{T}$ Known constant vector.

d'Dimension of decision variable vector.

Number of effective samples by strategic

sampling.

Dimension of the random variable vector. Estimated numbers of scenarios by diverse

random sampling-based methods.

The i'-th state (sample).  $st_{i'}$ Action from  $st_{i'}$  to  $st_{i'}$ .  $at_{i'j'}$ 

Transition probability from  $st_{i'}$  to  $st_{i'}$ .  $\pi_{i'i'}$ Reward function from  $st_{i'}$  to  $st_{i'}$ .  $r_{i'j'}$ 

 $D_{i'i'}$ Dissimilarity of two samples (scenarios).

Potential state set for next state.

Symmetric indefinite matrices for  $P_{i,t}$ ,  $Q_{i,t}$ .  $A_{ij}, B_{ij}$ Symmetric indefinite matrices for  $P_{ii,t}$ ,  $Q_{ii,t}$ .

1949-3053 © 2021 IEEE. Personal use is permitted, but republication/redistribution requires IEEE permission. See https://www.ieee.org/publications/rights/index.html for more information.

M

 $X_t$ 

 $X_{ij,t}$ 

M'	Number of coefficients.
$\mu$	Tunable regularization parameter.
Variables	
$P_{i,t}^g, \mathcal{Q}_{i,t}^g \ P_{i,t}^{net}, \mathcal{Q}_{i,t}^{net}$	Generator active and reactive power. Net active and reactive power inputs of PLREG.
$egin{aligned} e_{i,t} \;, f_{i,t} \ P_{ij,t},  Q_{ij,t} \end{aligned}$	Real and imaginary parts of bus voltage. Active and reactive power flow at lines.
$P_{ES,i,t}, \ Q_{ES,i,t} \ P_{ES,i,t}^{loss}$	Active and reactive power of energy storage. Active power loss of energy storage.
$V_{i,t}^{ES,i,t} \ P_{ES,i,t}^{net}$	Square of voltage magnitude. Net active power of energy storage.
$P_{i,t(base)}^{g}$ $Q_{i,t(base)}^{g}$	Base part of the generator's active power.
$Q_{i,t(base)}^{g}$ $P_{ES,i,t(base)}$	Base part of the generator's reactive power.  Base part of the energy storage's active power.
$Q_{ES,i,t(base)}$	Base part of the energy storage's reactive power.
у	Variable vector consisting of the decision variables and the state variables.
δ	Random variable vector of the net active and reactive power inputs.
v	Decision variable vector.
$A_i^*, A_{ij}^*$	Positive semi-definite (PSD) coefficient matrices of the quadratic terms.
- ste - ste	0 00 1

Training sample size.

#### I. Introduction

Constant terms.

or reactive power.

Auxiliary variable.

Coefficient vectors of the linear terms.

Voltage component vector at all buses.

Upper index set  $\{p, q\}$  indicating the active

Voltage component vector at *i*-and *j*-th buses.

Real NERGY storage (ES) has been well-recognized for dealing with the challenges in power systems, such as shaving peak-load and filling valley-load. However, the current cost of battery ES is still expensive. According to the roadmap of ES issued by the U.S. department of Energy in 2020, by 2030 the levelized cost of battery ES may be reduced to only 10% of the current cost [1]. This probably makes ES widely used in power systems. However, the inter-temporal property of ES may couple the multi-period power system operation (PSO). Moreover, the intermittence of renewable energy (RE) brings the uncertainty to PSO. Hence, the exploration on optimizing the multi-period PSO with ES (PSO-ES) under the uncertainty of RE is rather challenging. Unfortunately, the current deterministic approaches are incapable of capturing the uncertainty in the context of optimization. There exist some approaches of modeling optimization problems under uncertainty, such as stochastic, robust, and chance-constrained optimization methods [2]–[7]. The stochastic optimization [2], [3] attempts to find solutions with the best expected objective values based on the predefined probability distributions. The robust optimization [3], [4] enforces strict feasibility under the worst

case, resulting in high conservativeness. Unlike the two methods above, the chance-constrained optimization (CCO) [5]–[7] can guarantee that the satisfactory probability of a solution is above a certain level if properly implemented. Generally, power system operators put higher weight in security than in cost-saving. As a tradeoff, power operators may be more interested in solutions with the low probability of constraint violation. Therefore, in this paper, CCO is adopted to model the multi-period PSO-ES problem under uncertainty (CC-PSO-ES). For solving the CCO problems, the conventional methods generally assume a probability distribution (PD) on the uncertain variables, such as the power load and renewable energy generation (PLREG), and enforce the constraints to satisfy a desired level of probability, i.e., confidence level. We call the conventional methods as PD-based methods. However, such methods turn out to be computationally expensive for several reasons [8]-[11]. First, the actual joint PD of uncertain variables may be hard to access in some cases. Even if the actual joint PD is available, converting the probabilistic constraints to the deterministic constraints by the multivariate integral is computationally prohibitive and cannot guarantee the converted deterministic constraints are convex. Second, Monte Carlo-based method may be the only way to check whether a specific point of decision variables satisfies the probabilistic constraints, and it is too costly when setting a high confidence level. In addition, the discussions on the solution methods of the CCO problems in many existing references [5]-[7] mainly depend on the strict assumptions that all uncertain variables are independent and the actual joint PD is tractable.

As an alternative to the PD-based methods to solve the CCO problems, the PD-free methods, called scenario optimization or scenario-based methods, don't rely on the actual PD of uncertainty, but only use the historical scenarios of uncertainty. Such methods have been applied in probabilistic optimization problems [12]-[18] learning models and artificial intelligence (AI) [19]–[21]. The scenario optimization determines the minimum sample size (MSS) that is required to satisfy the specific probability level [12]-[14]. Reference [13] illustrates a random sampling (RS)-based method (RSM) to estimate the MSS associated with the number of decision variables under the convex program. To verify the efficacy of RSM, [15]–[18] exemplify the utilization of the scenario-based solution methods in economic dispatch and reserve scheduling considering the uncertainty of demand response or renewable energy generations. The method in [17], [18] adjusts the level of conservativeness of solutions by discarding samples, but it is computationally expensive in complex systems as discarding samples needs to solve the optimization problem repeatedly. Additionally, for complex systems with numerous decision variables, the MSS estimated by RSM may explode as the MSS grows with the size of decision variables [13]. To tackle this issue, the fast algorithm for scenario technique (FAST), a two-stage method [14] has been proposed to cut down the sample size and applied in computing optimal power flow with uncertainty [22]. As stated in RS-based methods [9], [10], [13], [14], [17], [18] in convex programs there may have a small size of 'active' scenarios that essentially decide the optimal solution. The number of active scenarios is proven to be at most the decision variable size, which is far smaller than the sample size determined by RSM. In other words, there exist abundant repetitive or similar scenarios via RSM. However, these active scenarios are unknown before solving the CCO problems using RSM. Inspired by the resounding sequential sampling [19], [20] used in machine learning and the existence of physical patterns in data, a concept of strategic sampling is developed in this paper to find a much smaller size of effective scenarios that can approximate the effect of the active scenarios before optimization, through physics-guided sampling [23], [24], dissimilarity-based learning [25] and reinforcement learning [26]–[29] methods.

The above-mentioned scenario-related optimization methods are mostly applied in convex program problems [13], [14]. However, the constraints of AC power flow (ACPF) in CC-PSO-ES problem are inherently nonlinear and nonconvex [6]. Currently, the approximations of ACPF have been discussed from the perspectives of linearization and convexification. The linear approximations like the DC model [7], [30] and other linear ACPF [6], [31], are generally easy to solve, however, many of which ignore the quadratic terms of voltages resulting in inaccuracy of model. The typical convex approximations have been widely studied, such as the second-order cone (SOC) [32], semidefinite programming (SDP) [33], convex DistFlow [34], quadratic convex (QC) [35], moment-based [36], convex hull relaxation [37], and the learning-based convex approximation [38], [39]. References [39]-[41] found that the SDP relaxation may not guarantee the exactness of solutions and its exactness greatly depends on the critical assumptions of network topologies and physical parameter settings. In [39], the authors developed an ensemble learning-based data-driven convex quadratic approximation (DDCQA) of ACPF with higher accuracy and efficiency than the SDP relaxation. This paper introduces the generalized least absolute shrinkage and selection operator (LASSO) [42]–[45] to improve the DDCQA developed in [39] from both aspects of the computing time and memory used. LASSO is one of the most popular methods for selection and estimation of parameters in regression problems [42], [43]. It is used for not only the variable selection, but also the parameter regularization. Unlike the forward and backward selection methods that yield the local optimal results, LASSO is formulated as a convex problem that outputs the global optimal result [44]. The generalized LASSO exhibits the superiority over LASSO in the stability and the speed of computation [45], which is adopted to learn sparser coefficient matrices in the current research.

To solve the CC-PSO-ES which is a complex multi-period nonlinear nonconvex optimization problem, this paper proposes a novel scenario-based solution method based on the DDCQA of ACPF and strategic sampling. The proposed approach is more computationally effective using only few effective scenarios, compared with RSM. The contributions of this paper are written as below:

1) Unlike the existing PD-based methods to solve the CCO problems, the proposed solution method based on two-stage hybrid sampling (HS) is PD-free and use the historical samples

of uncertainty. HS makes full use of the physical patterns of data and the merits of learning algorithms. The innovation of HS resides in using the resounding learning algorithms to improve the sampling effect and computational efficiency, avoiding the repetitive samples using dissimilarity metric and preserving the accuracy of solution. There are few existing references discussing HS for the PD-free solution paradigm of CCO. To the best of our knowledge, the existing work on the PD-free solution paradigm of CCO generally uses random sampling (RS) [9], [10], [13]–[18].

2) The DDCQA of ACPF is significantly improved by the generalized LASSO from the aspects of computational time and memory usage, then applied to convert the originally intractable nonconvex CC-PSO-ES problem into a tractable convex quadratic optimization problem.

The rest of this paper is organized as follows: Section II illustrates the formulations of deterministic and chance-constrained multi-period PSO-ES problems. In Section III, scenario optimization is introduced, and the novel scenario-based solution method for CC-PSO-ES problem is developed by strategic sampling and the DDCQA of ACPF modified by generalized LASSO. The empirical IEEE case analyses and conclusions are displayed in Sections IV and V, respectively.

#### II. PROBLEM FORMULATION

This section formulates the optimal multi-period operation for power systems with energy storage under the modeling paradigm of chance-constrained optimization step-by-step.

# A. Deterministic Multi-Period PSO With Battery Energy Storage

In an *n*-bus power system, the deterministic formulation of the multi-period PSO-ES is given below which can be considered as a multi-period AC optimal power flow (ACOPF) with adjustable generations and battery energy storages:

$$\begin{aligned} & \textit{Min } \sum_{t \in T'} \sum_{i} \left( c_{i1} P_{i,t}^g + c_{i2} (P_{i,t}^g)^2 \right) & \text{(1a)} \\ & \textit{s.t. } e_{i,t} \sum_{j=1}^{n} \left( G_{ij} e_{j,t} - B_{ij} f_{j,t} \right) + f_{i,t} \sum_{j=1}^{n} \left( G_{ij} f_{j,t} + B_{ij} e_{j,t} \right) \\ & = P_{i,t}^g - P_{i,t}^{net} + P_{ES,i,t} & \text{(1b)} \\ & f_{i,t} \sum_{j=1}^{n} \left( G_{ij} e_{j,t} - B_{ij} f_{j,t} \right) - e_i \sum_{j=1}^{n} \left( G_{ij} f_{j,t} + B_{ij} e_{j,t} \right) \\ & = Q_{i,t}^g - Q_{i,t}^{net} + Q_{ES,i,t} & \text{(1c)} \\ & G_{ij} e_{i,t} e_{j,t} - B_{ij} e_{i,t} f_{j,t} + B_{ij} f_{i,t} e_{j,t} + G_{ij} f_{i,t} f_{j,t} \\ & - G_{ij} \left( e_{i,t}^2 + f_{i,t}^2 \right) = P_{ij,t} & \text{(1d)} \\ & G_{ij} f_{i,t} e_{j,t} - B_{ij} e_{i,t} e_{j,t} - G_{ij} e_{i,t} f_{j,t} - B_{ij} f_{i,t} f_{j,t} \\ & + B_{ij} \left( e_{i,t}^2 + f_{i,t}^2 \right) = Q_{ij,t} & \text{(1e)} \end{aligned}$$

$$P_{ES,i,t}^{loss} V_{i,t}^2 = r_i^{eq} P_{ES,i,t}^2 + r_i^{cvt} Q_{ES,i,t}^2$$
 (1f)

$$P_{ES,i,t}^{net} = P_{ES,i,t} + P_{ES,i,t}^{loss}$$
 (1g)

$$P_{ES,i,t}^2 + Q_{ES,i,t}^2 \le S_{ES,i}^{max^2}$$
 (1h)

$$E_{ES,i}^{min} \le E_{ES,i,0} + \Delta t \sum_{k=1}^{t} P_{ES,i,k}^{net} \le E_{ES,i}^{max}$$
 (1i)

$$V_{i,t}^{min2} \le e_{i,t}^2 + f_{i,t}^2 \le V_{i,t}^{max2} \tag{1j}$$

$$P_{i,t}^{gmin} \le P_{i,t}^g \le P_{i,t}^{gmax} \tag{1k}$$

$$Q_{i,t}^{gmin} \le Q_{i,t}^{g} \le Q_{i,t}^{gmax}$$

$$P_{ij,t}^{2} + Q_{ij,t}^{2} \le S_{ii,t}^{gmax}$$
(11)

$$P_{ij,t}^2 + Q_{ij,t}^2 \le S_{ii,t}^{gmax} \tag{1m}$$

The equations (1a)-(1m) illustrates a deterministic model for multi-period power system operation (PSO) with battery energy storage. The equation (1a) indicates the objective function that minimizes the total PSO cost. The constraints of power balance are presented in (1b)-(1c). The equations (1d)-(1e) denotes the constraints of power flows at power lines. The formulations for battery energy storages (BES) are represented in (1f)-(1i) considering the power loss of BES. The equations (1j)-(1m) are used to bound the bus voltages, active(reactive) power injections and transmission capacities.

## B. Chance-Constrained Formulation of Multi-Period PSO With Adjustable Generation and Battery Energy Storage

Considering that the net load inputs of PLREG are random variables, the power generation may be fluctuating, which consists of the base and adjustable parts. The base part meets the forecast net demand injection of PLREG. The gap between the forecast and actual net demand injections is satisfied by the adjustable part. According to the affine control scheme [46], then

$$P_{i,t}^{net,s} = P_{i,t(frt)}^{net} + \Delta p_i^s \tag{2a}$$

$$\begin{aligned} P_{j,t}^{net,s} &= P_{j,t(frt)}^{net} + \Delta p_j^s \\ Q_{j,t}^{net,s} &= Q_{j,t(frt)}^{net} + \Delta q_j^s \end{aligned} \tag{2a}$$

$$P_{i,t}^{g,s} = P_{i,t(base)}^g - \omega_{pi} \sum_{j=1}^n \Delta p_j^s$$
 (2c)

$$Q_{i,t}^{g,s} = Q_{i,t(base)}^g - \omega_{qi} \sum_{j=1}^n \Delta q_j^s$$
 (2d)

$$P_{ES,i,t}^{s} = P_{ES,i,t(base)} - \omega_{pi} \sum_{j=1}^{n} \Delta p_{j}^{s}$$
 (2e)

$$Q_{ES,i,t}^{s} = Q_{ES,i,t(base)} - \omega_{qi} \sum_{j=1}^{n} \Delta q_{j}^{s}$$
 (2f)

$$\sum_{i} \omega_{pi} + \sum_{i} \omega_{pj} = 1 \tag{2g}$$

$$\sum_{i} \omega_{qi} + \sum_{i} \omega_{qj} = 1 \tag{2h}$$

Note that we assume the difference between the base case and real-time power loss can be compensated by the reference generator and it is typically negligible. Suppose that the chance-constrained method is used to model the problem (1) under uncertainty. Then, by substituting  $(2a)\sim(2h)$  into (1) and updating each variable in (1) with the superscript s, the deterministic problem (1) is reformulated into a CC-PSO-ES problem in (2):

$$\min_{s \in S'} E \left[ \sum_{t \in T} \sum_{i} \left( c_{i1} P_{i,t}^{g,s} + c_{i2} \left( P_{i,t}^{g,s} \right)^{2} \right]$$
 (2i)

$$s.t. \ h(y,\delta) = 0 \tag{2j}$$

$$Pr(f(y, \delta) \le 0) \ge 1 - \alpha$$
 (2k)

where  $h(y, \delta)$ ,  $f(y, \delta)$  compacts the constraints of (1b) $\sim$ (1h) and (1i) $\sim$ (1m), respectively;  $Pr(\cdot)$  enforces each constraint at a specific confidence level.

# III. A SCENARIO-BASED SOLUTION METHOD WITH STRATEGIC SAMPLING AND DATA DRIVEN CONVEX APPROXIMATION

#### A. Scenario Optimization

Scenario optimization has been widely used in machine learning [13], [14], [19], [20], whose general idea is to use a finite number of scenarios to approximate the probabilistic constraints (2j) and (2k) with a specific confidence level. The mathematical formulation can be represented as

$$Min \ C^T v$$
 (3a)

s.t. 
$$F(v, \delta^{(s)}) \le 0$$
,  $(s = 1, 2, ..., N' \in S')$  (3b)

where (3a) is a linear objective function related to the decision variable vector v;  $\delta^{(s)}$  denotes the s-th scenario sampled from the uncertainty set; F is a convex function on v; N' is the estimated number of scenarios. In the existing applications of scenario optimization, the constraints depend upon the random samples, and the sample size discussed in the statistical learning [20], [21] has a conversative estimate unrelated to the number of decision variables. Until in [13], the lower bound of the sample size related to the decision variable size under convex program settings is derived from the aspect of binomial distribution. A theorem in [13] states that, if N' is sufficiently large, the optimal solution of (3) can satisfy the chance constraints  $(2i)\sim(2k)$ . Scenario optimization is still an emerging solution method for chance-constrained optimization that does not rely on the assumed PD [12]-[18]. The RS-based method in [13]-[18] provides some discussions on how to determine the required number of scenarios, shown in (3c):

$$N' \ge \frac{2}{\epsilon} \left( \ln \frac{1}{\beta} + d' \right) \tag{3c}$$

However, in CC-PSO-ES problem, the number of scenarios required by the RS-based method may be very large, which results in significant challenge in optimization computation. Moreover, scenario optimization is applied in convex programs [13]-[18], while there have nonconvex constraints in current CC-PSO-ES problem. Hence, the following sections will discuss how to tackle the two issues through the strategic sampling and DDCOA, respectively.

# B. Strategic Sampling

Instead of random sampling with plentiful inactive scenarios [13]–[18], we attempt to develop a framework of strategic sampling to find out a smaller number of effective scenarios

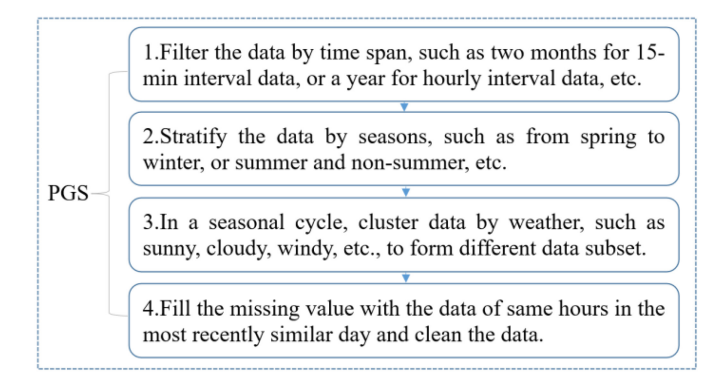


Fig. 1. Flowchart of Physics-guided Sampling.

that include the active ones. According to different selection strategies, there may have diverse specific strategic sampling methods, such as physics-guided sampling (PGS) [23], [24], learning-based sampling, and hybrid sampling, etc., [25]–[29]. The PGS is designed considering there might have specific patterns in PLREG data. The patterns may be related to the temporal, spatial, and meteorological conditions [23], [24]. The learning-based sampling is based on machine learning methods, such as dissimilarity-based learning [21] and reinforcement learning (RL) [26]–[29]. The hybrid one may be the combination of any two sampling methods. In this research, two types of two-stage hybrid sampling methods are developed and named as HS1 and HS2. The first stage is the physicsguided sampling (PGS). Then, at the second stage, i.e., the stage of learning-based sampling, one of dissimilarity-based sampling (DBS) and RL-based sampling (RLS) will be chosen to select the d dissimilar samples. From a series of experimental simulations, in IEEE-5 system, d is suggested to be at least the number of the decision variables; in IEEE-9, -57, and -118 systems we can set d to be 10%-15% of the number of decision variables.

- 1) Physics-Guided Sampling: Assume there are regional power systems like IEEE-5, -9, -57, -118 systems. The gist of PGS for a specific regional power system can be described in Fig. 1 [23], [24].
- 2) Dissimilarity-Based Sampling: The dissimilarity-based sampling (DBS) is defined to use a learning function to select the scenarios. The purpose of using a learning function is to ensure that the scenarios selected should be dissimilar enough to maximize the scenario difference in a specific data subset obtained after PGS. To measure the dissimilarity of samples, in machine learning the distance metrics are commonly used, such as the Euclidean distance [19], [25]. Assume that  $\delta_{i'}$ ,  $\delta_{j'}$  are the i'-th and j'-th samples where  $\delta_{i'} = (\delta_{i'}^1, \delta_{i'}^2, ..., \delta_{i'}^m)$ ; m is the dimension of each sample. The dissimilarity between two samples can be measured by the Euclidean distance calculated as

$$D_{i'j'} = \sqrt{\sum_{k=1}^{m} \left(\delta_{i'}^{k} - \delta_{j'}^{k}\right)^{2}}$$
 (4a)

where  $D_{i'j'}$  denotes the dissimilarity of two samples, used for determining the new samples. The specific hybrid sampling

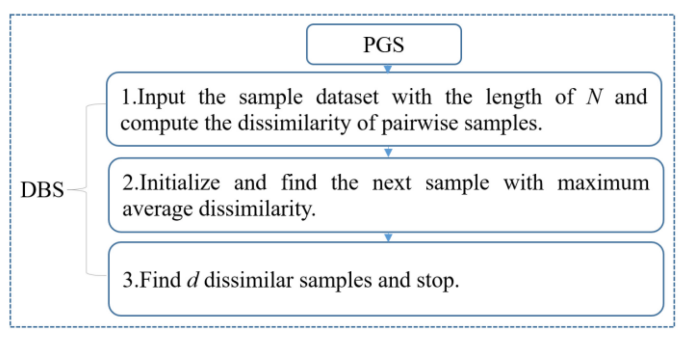


Fig. 2. Flowchart of Hybrid Sampling Type 1 (HS1).

that consists of PGS and DBS is described as HS1 in Fig. 2 where *N* is computed by FAST [14].

3) Reinforcement Learning-Based Sampling: In essence, RL involves a Markov decision process (MDP). A MDP consists of the state space, the action space, the transition function, and the reward function. The transition probability from the current state to next state is only decided by the current state in a MDP. The action from the current state to next state will be rewarded according to the reward function. The objective in a MDP is to find an optimal policy to maximize the expected cumulative reward [27]. In this paper, the model-based RL algorithm [26]–[29] is adopted to develop the sampling method. In this version of RL algorithm, the models of the transition and reward functions are known or learned, and then perform the value or policy iteration to yield the optimal policy, corresponding to a small set of effective samples in this paper. The RL-based sampling (RLS) is used to search a small set of dissimilar (effective) samples from the input sample dataset with finite samples. Specifically, we consider each sample as a state  $st_{i'}$ , and the transition function  $\pi_{i'i'}$ , i.e., the transition probability from the i'-th state  $st_{i'}$  to j'-th state  $st_{i'}$  by the action  $at_{i'i'}$  is defined as:

$$\pi_{i'j'}(st_{j'} \mid st_{i'}, at_{i'j'}) = \frac{D_{i'j'}}{\sum_{j' \in H} D_{i'j'}}$$
 (4b)

where the indices i' and j' correspond to the current and next state; H is the potential state set for next state. The reward function  $r_{i'j'}$  of the transition from the i'-th state to j'-th state is defined to be  $D_{i'j'}$ , and the discount factor of reward is set to one in this research. Based on the known transition and reward functions above, the value or policy iteration can be used to yield the optimal policy, namely, a map of states to actions, corresponding to the dissimilar samples in this paper. To prevent the agent from repeating a state multiple times, after each transition, the previous states traversed will be removed from the potential state set. In this fashion, the agent will try to select the action directing to the 'farthest' state (sample) with the maximum dissimilarity in the potential state set. To some extent, the defined transition and reward functions can circumvent the instability from learning them and using the dissimilarity metric can reduce the instability due to the correlations existing in the samples [27]–[29]. The implementation of RLS is shown as HS2 in Fig. 3. The main difference between DBS and RLS lies in that RLS only consider the

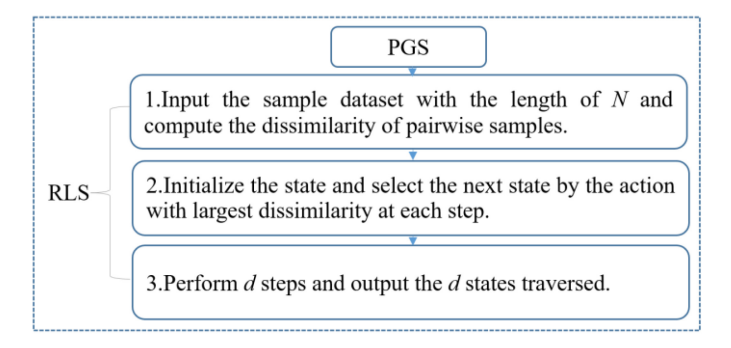


Fig. 3. Flowchart of Hybrid Sampling Type 2 (HS2).

dissimilarity between the current selected sample and the candidate sample, while DBS computes the average dissimilarity between the previous all selected samples and the candidate sample.

The proposed sample selection strategies are reasonable for the following reasons. First, stated in [9], [10], [13], [14], [17], [18] in convex programs only a small set of 'active' scenarios (samples) decides the optimal solution and there are many repetitive or similar scenarios selected by RSM [9], [10], [13], [14]. For instance, for randomly sampling I samples, assume a scenario u(s) has the probability Pr(u(s)), then it may be sampled I\*Pr(u(s))times. However, for optimization problems, only one u(s) is sufficient and the rest of (I\*Pr(u(s))-1) ones are unnecessary. The proposed hybrid sampling (HS) methods can avoid these repetitive or similar scenarios and only keep a small number of diverse scenarios that can approximate the effect of active scenarios, because of using the dissimilarity metric. Many learning methods distinguish samples by their dissimilarities or similarities [47]-[49], inspiring us to design DBS and use the dissimilarity metric to guide the agent's action in RLS. Second, the specific physical patterns do exist in power and energy data, such as the temporal, spatial and meteorological patterns. From this point, it would be advisable to design the physics-guided sampling.

# C. Data-Driven Convex Quadratic Approximation of Power Flow

Note that the scenario-based solution methods discussed so far are designed for the convex program [12]–[18], while, in the original CC-PSO-ES problem, the constraints of ACPF are nonconvex. To deal with the issue of nonconvexity, we improve the data-driven convex quadratic approximation (DDCQA) of ACPF [39] using the generalized LASSO [42]–[45]. For the ease of analysis, the constraints (1b)-(1e) at *t*-th hour are reformulated as the following matrix form:

$$P_{i,t} = X_t^T A_i X_t (5a)$$

$$Q_{i,t} = X_t^T B_i X_t \tag{5b}$$

$$P_{ij,t} = X_{ij,t}^T A_{ij} X_{ij,t}$$
 (5c)

$$Q_{ij,t} = X_{ij,t}^T B_{ij} X_{ij,t}$$
(5d)

$$X_t = [x_{1,t} \ x_{2,t}, ..., x_{2n,t}]^T = [e_{1,t} \ f_{1,t}, ..., e_{n,t} \ f_{n,t}]^T$$
 (5e)

$$X_{ij,t} = \begin{bmatrix} x_{2i-1,t} & x_{2i,t} & x_{2j-1,t} & x_{2j,t} \end{bmatrix}^T = \begin{bmatrix} e_{i,t} & f_{i,t} & e_{j,t} & f_{j,t} \end{bmatrix}^T$$
 (5f)

where  $A_i$ ,  $B_i$ ,  $A_{ij}$ ,  $B_{ij}$  are symmetric indefinite matrices consisting of elements of the admittance matrix, implying all dependent variables  $P_{i,t}$ ,  $Q_{i,t}$ ,  $P_{ij,t}$ , and  $Q_{ij,t}$  are nonconvex functions of the independent variables  $X_t$  or  $X_{ij,t}$ . Hence, a convex quadratic mapping (5g)-(5j) between power, i.e.,  $P_{i,t}$ ,  $Q_{i,t}$ ,  $P_{ij,t}$ , and  $Q_{ij,t}$ , and voltage  $X_t$  or  $X_{ij,t}$ , is defined as:

$$P_{i,t} = X_t^T A_i^p X_t + B_i^p X_t + c_i^p$$
 (5g)

$$Q_{i,t} = X_t^T A_i^q X_t + B_i^q X_t + c_i^q$$
 (5h)

$$P_{ij,t} = X_{ij,t}^T A_{ii}^p X_{ij,t} + B_i^p X_{ij,t} + c_{ii}^p$$
 (5i)

$$Q_{ii,t} = X_{ii}^{T} A_{ii}^{q} X_{ii,t} + B_{i}^{q} X_{ii,t} + c_{ii}^{q}$$
 (5j)

According to [39], the positive semi-definite (PSD) matrices  $A_i^p$ ,  $A_i^q$ ,  $A_{ii}^p$ ,  $A_{ii}^q$  in (5g)-(5j) can be obtained via training historical data using the polynomial regression as a basic learner to learn the convex relationships between the voltage and the active or reactive power. Then, ensemble learning methods are used to assemble all basic learners, to boost the performance of model. However, the PSD matrices in (5g)-(5j) are dense and high-dimensional, which is an obstacle in computing the complex CC-PSO-ES problem. Therefore, the generalized LASSO [42]-[45] is introduced to learn more compact and sparser PSD matrices for the purposes of speeding up the computational efficiency and saving the storage space. The following illustration of generalized LASSO takes  $P_{i,t}$  as an example based on dataset  $\{x_{it}, y_{it}\}_{i=1}^{M}$  where  $x_{it}, y_{it}$  are the *i*-th observed voltage input and active power output at t-th hour; M is the training sample size. The detailed formulation is

$$\min \frac{1}{M} \sum_{i=1}^{M} (y_{it} - X_t^T A_i^p X_t - B_i^p X_t - c_i^p)^2 + \mu \sum_{j=1}^{M'} |\theta_j| \quad (5k)$$
s.t.  $A_i^p \geq 0$  (51)

where  $\theta_j$  is the *j*-th coefficient constituted by the entries of  $A_i^p$ ; ' $\succcurlyeq$ ' means  $A_i^p$  is a PSD matrix; M'is the number of coefficients;  $\mu \ge 0$  is a tunable regularization parameter that controls the degree of shrinkage. By the shrinkage, some coefficients may be zero, which means the matrix  $A_i^p$  becomes sparse.

#### D. Convex Hull Relaxation of Energy Storage Model

As suggested by [50], it is a typical design requirement for AC power grids to design small phase angle differences and the voltage drop can be negligible in many systems [51]–[58]. The solutions of AC optimal power flow in IEEE test systems in [54], [55] also verify that the bus voltage magnitudes are approximate to 1.0 (p.u.). Besides, many LinDistFlow models [56]–[58] assume power line losses at any line segment are negligible and the voltage drop from the slack node to each node is sufficiently small. Hence, we assume that  $V_{i,t}^2 \approx 1.0$  (p.u.) in (1f) for the nodes with the energy storage. Then, the convex hull relaxation [37] of the energy storage model can be formulated as the followings:

$$||Jz_{i,t}||_2 - b^T z_{i,t} \le 0$$
 (6a)

$$||J_{i}z_{i,t}||_{2} - b^{T}z_{i,t} \le m_{i}$$
 (6b)

$$K_i^T z_{i,t} - 2m_i \le 0 (6c)$$

where 
$$J = diag([\sqrt{2} \sqrt{2} \ 1 \ 1]^T)$$
,  $b = [0 \ 0 \ 1 \ 1]^T$ ,  $J_i = diag([0 \ \sqrt{2r_i^{batt}} \ 1 \ 1]^T)$ ,  $z_{i,t} = [P_{ES,i,t} \ Q_{ES,i,t} \ P_{ES,i,t}^{loss} \ 1]^T$ ,  $K_i = [0 \ 0 \ r_i^{eq} \ S_{ES,i}^{max2}]^T$ ,  $m_i = r_i^{eq} S_{ES,i}^{max2}$ .

## E. Scenario Programming Formulation of CC-PSO-ES

Based on the DDCQA of power flow constraints in (5g)-(5j) and the convex hull relaxation of energy storage model in (6a)-(6c), the corresponding convex constraints are written as

$$X_{t}^{T} A_{i}^{p} X_{t} + B_{i}^{p} X_{t} + c_{i}^{p} \le P_{i,t}^{g} - P_{i,t}^{net} + P_{ES,i,t}$$
 (7a)

$$X_t^T A_i^q X_t + B_i^q X_t + c_i^q \le Q_{i,t}^g - Q_{i,t}^{net} + Q_{ES,i,t}$$
 (7b)

$$X_{ij,t}^{T} A_{ij}^{p} X_{ij,t} + B_{i}^{p} X_{ij,t} + c_{ij}^{p} \le P_{ij,t}$$
 (7c)

$$X_{ij,t}^{T} A_{ij}^{q} X_{ij,t} + B_{i}^{q} X_{ij,t} + c_{ij}^{q} \le Q_{ij,t}$$
 (7d)

$$x_{2i-1,t}^2 + x_{2i,t}^2 \le V_{i,t}^{max2}$$

$$(1k) - (1m)$$
 and  $(6a) - (6c)$ . (7e)

Then, we introduce an auxiliary variable Z used to reformulate the objective function (2i) into a linear formulation (7f) with a convex constraint (7g) as

Minimize: 
$$Z$$
 (7f)

s.t. 
$$\sum_{s \in S'} \sum_{t \in T} \sum_{i} \left( c_{i1} P_{i,t}^{g,s} + c_{i2} (P_{i,t}^{g,s})^2 \right) \le |S'| Z \quad (7g)$$

where |S'| is the number of scenarios. As the constraints above are all convex, the scenario programming, i.e., the strategic sampling-based solution approach for the CC-PSO-ES problem can be rewritten in (8) as

Minimize: 
$$(7f)$$
 (8a)

s.t. 
$$F'(y, \delta^{(s)}) \le 0$$
,  $(s = 1, 2, ..., d)$  (8b)

where  $F'(y, \delta)$  compacts all constraints in (7a)-(7e), (7g), (1k)-(1m), and (6a)-(6c) at each scenario. The corresponding sampling procedure for the problem (8) is illustrated in the section of strategic sampling.

#### IV. SIMULATION ANALYSIS

### A. Case Selection and Data Collection

The real-world power systems and their data are expected to use in this research. However, they are not available in public. As empirical alternatives, some IEEE standard test systems such as IEEE-5, -9, -57, and -118 systems studied in [40], [54] are used and the steady-state operation conditions in these systems are preserved. The demand data is accessed from ISO New England [59]. The net active and reactive power loads at each bus are based on the hourly load curves of ISO new England and set up at the range of [0.7, 1.3] of their true values to simulate the uncertainty of power loads and renewable energy generations and to generate the 24-hour simulating data. The settings of energy storage units are summarized in Table I [37]. Considering sampling in the whole sample space may be computationally expensive, for each test system, the sample size determined by the RS-based method [13]–[18] is treated as the sample space. The goal is to demonstrate the efficacy of the proposed solution method with fewer effective scenarios via the strategic sampling methods

TABLE I SETTINGS OF ENERGY STORAGE UNITS

Case	IEEE-5	IEEE-9	IEEE-57	IEEE-118
Units	2	2	3	3
Bus No.	3,5	5, 7	8, 9, 12	59, 90, 116
- C :	1MVA,	0.75MVA,	0.75MVA,	1MVA,
Capacity	2MWh	1.5MWh	1.5MWh	2MWh

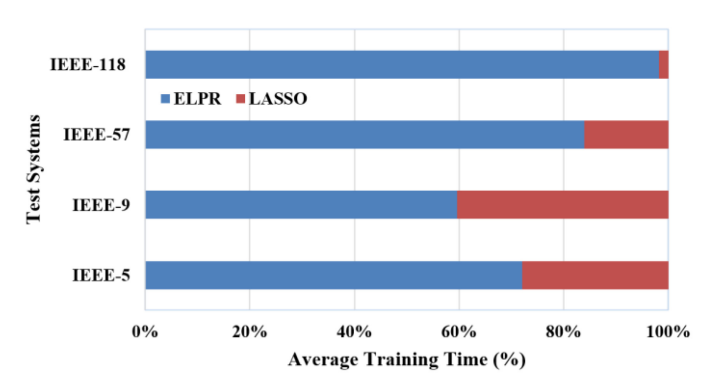


Fig. 4. Comparison of Training Time.

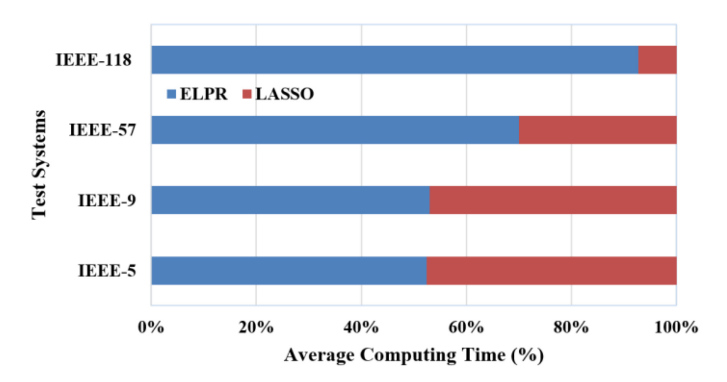


Fig. 5. Comparison of Computing Time of CC-PSO-ES.

and the DDCQA of ACPF. The simulations are performed in MATLAB with cvx package.

#### B. Computational Complexity Comparison of DDCQA

To compare the computational efficiency of the DDCQA of ACPF before and after improvement, we explore the average training time for the active and reactive power at each bus and the average computation time for solving the CC-PSO-ES problems, using the existing method, i.e., ensemble learning-based polynomial regression (ELPR) [39], named as 'ELPR' and the generalized LASSO named as 'LASSO', shown in Figs. 4-5. Figs. 4 and 5 indicate that there exist significant improvements in both the training time and computing time of CC-PSO-ES problem, using 'LASSO' instead of 'ELPR'. Particularly, on IEEE-57 system, it only takes about 25% of the original average training time to train the improved DDCOA and about 40% of the original average computing time of CC-PSO-ES to obtain the solution. For the IEEE-118 system, the average training time and the average computing time of CC-PSO-ES used now are only about 2% and 5% of the ones before, respectively. As the supplements of Figs. 4 and 5, the specific

TABLE II AVERAGE TRAINING TIME (UNIT: SECOND)

Case	ELPR	LASSO	Runtime Reduction
IEEE-5	0.98	0.38	61.22%
IEEE-9	1.02	0.69	32.35%
IEEE-57	3.96	0.76	80.81%
IEEE-118	53.77	1.01	98.12%

TABLE III
AVERAGE TIME OF COMPUTING CC-PSO-ES (UNIT: SECOND)

Case	ELPR	LASSO	Runtime Reduction
IEEE-5	11.38	10.32	9.31%
IEEE-9	22.10	19.64	11.13%
IEEE-57	2837.72	1214.31	57.21%
IEEE-118	36767.43	2875.22	92.18%

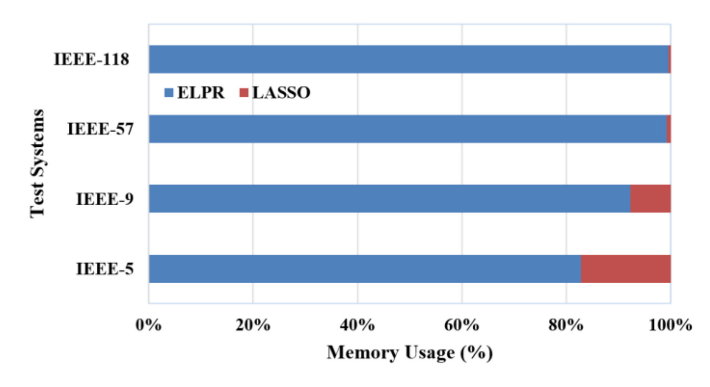


Fig. 6. Comparison of Memory Usage.

data of average training time and average time of computing CC-PSO-ES problems are provided in Tables II and III where the runtime reduction in the two tables is computed by (1-runtime(LASSO)/runtime(ELPR))\*100%. Both Figs. 4, 5 and Tables II, III conclude that 'LASSO' spends less time than 'ELPR' on training the DDCQA and computing the CC-PSO-ES problem. Specifically, there are 30%-98% and 9%-90% runtime reductions for training the DDCQA and computing the CC-PSO-ES problem, respectively.

Moreover, the memory usages of the matrix  $A_i^p$  before and after improving DDCQA in all test systems have been displayed in Fig. 6. This figure shows that in all test systems, the memory usage consumed now is reduced by over 75% compared with the one consumed before. For IEEE-57 and -118 systems, the memory usage used now may only account for 1%-2% of the one used before. Overall, the improved DDCQA based on the generalized LASSO greatly decreases the computational complexity in training and computing the optimization problem.

In addition, the comparison between the generalized LASSO and other variable selection methods is performed. The results of ridge regression (RR) and forward / backward / 'both' selection methods have been provided and compared with the generalized LASSO. Note that RR in essence doesn't do variable selection but only shrink the magnitude of coefficients, and 'both' selection method mentioned means using both

TABLE IV

COMPARISON OF THE RESULTS OF VARIABLE SELECTION METHODS

(UNIT: P.U.)

Case		LASSO	Ridge	Forward	Backward	Both
IEEE-5 size=100	$P_i$	0.003812	0.071646	0.0904038	0.090405	0.090404
	$Q_i$	0.035367	0.047281	0.0785919	0.078583	0.078591
IEEE-9	$P_i$	0.002811	0.013257	0.0977825	0.097798	0.097780
size=100	$Q_i$	0.006885	0.026002	0.1976358	0.197632	0.197635
IEEE-57	$P_i$	0.004328	0.012902	0.0232383	0.023238	0.023237
size=200	$Q_i$	0.016140	0.020047	0.0331035	0.033102	0.033102
IEEE-118 size=300	$P_i$	0.003752	0.008019	0.0131902	0.013185	0.013181
	$Q_i$	0.012413	0.015748	0.0244099	0.024407	0.024405

Case	IEEE-5	IEEE-9	IEEE-57	IEEE-118
Objective Cost (\$/h)	477487	262187	296260	3603450

TABLE VI SAMPLE SIZES OF FAST AND RSM

Case	IEEE-5	IEEE-9	IEEE-57	IEEE-118
d'	864	1104	5904	17328
N	1050	1290	6090	17514
N'	34929	44529	236529	693489
Ratio $1 = d'/N'$	0.02474	0.02479	0.02496	0.02499

forward and backward selection methods. The average test errors denoted by the root-mean-square error (RMSE) for the active and reactive power  $P_i$  and  $Q_i$  at all buses under different variable selection methods are shown in Table IV (unit: p.u.). From this table, we can observe that: 1) the generalized LASSO and RR work better than forward / backward / both selection methods in learning the DDCQA in this manuscript; 2) the generalized LASSO has the best performance; 3) forward/backward/both selection methods have very similar performance.

# C. Performance Comparison of Solution Methods

In this numerical experiment, we set the allowed violation probability level and the confidence level to be  $\epsilon=0.05$  and  $1-\beta=0.9999$ , respectively. FAST [14] is used to provide a benchmark result. Both FAST and the proposed solution method based the strategic sampling can achieve the same objective costs of the CC-PSO-ES problems considering the uncertainty of PLREG, shown in Table V. This indicates that the proposed solution method achieves the optimal solutions of the CC-PSO-ES problems in our research. To compute the objective costs in TABLE V, the estimated number of scenarios required by the RS-based method (RSM) [13], [15]–[18] and FAST [14] are shown as N' and N, in TABLE VI where d' is the decision variable size.

TABLE VI shows that the number of active scenarios only accounts for at most 2.5% of the sample size computed by the

Case	IEEE-5	IEEE-9	IEEE-57	IEEE-118
RLS(best)	223	2	4	2
RLS(worst)	883	114	729	1780
DBS(best)	3	2	3	2
DBS(worst)	432	96	289	1661

RSM, reflected in the row of Ratio1. In other words, the majority of N' samples may be useless for solving the CC-PSO-ES problems. Compared with the RSM, FAST can reduce the number of scenarios to from N' to N. Especially, for IEEE-57 and -118 systems, the sample sizes required by the RSM are more than 230k and 690k, respectively. It will be difficult to solve the CC-PSO-ES problems with such large number of scenarios in practice. From TABLE VI, with the same confidence level requirement, it is easier to solve the CC-PSO-ES problems with N samples by FAST than with N' samples by the RSM, but it is still computationally expensive to compute the CC-PSO-ES problems in IEEE-57 and -118 systems. As a promising alternative of the RSM and FAST, the solution method via the strategic sampling, namely, the hybrid sampling methods via RLS and DBS, is illustrated below.

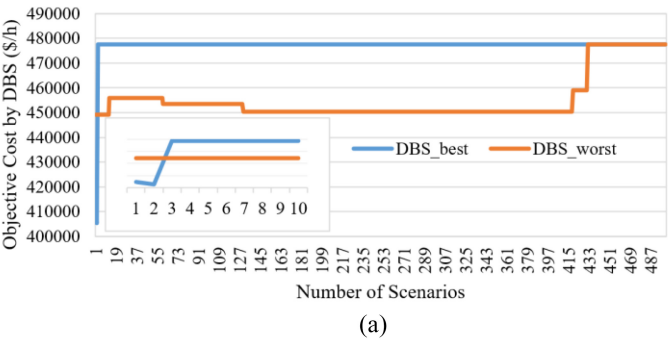
Similarly, for achieving the objective costs in Table V by the proposed solution method based on the DBS and RLS, the sample sizes required by DBS and RLS are shown in Table VII where the 'best' and 'worst' items correspond to the best and worst sample sizes selected by DBS and RLS based on many times of experimental simulations. From Table VII, we can infer that:

- 1) The sample selection results of HS1 and HS2 can be approximately bounded by the size of decision variables.
- 2) The hybrid sampling methods through DBS and RLS, i.e., HS1 and HS2, use far fewer samples than the RSM and FAST for solving the CC-PSO-ES problems, especially in IEEE-57 and -118 systems. For instance, in IEEE-5 system the solution methods via HS1 and HS2 find the optimal solution within 450 and 890 scenarios, respectively, which is smaller than 1050 scenarios determined by FAST. In a similar fashion, in IEEE-9, -57 and -118 systems, 120, 800 and 1800 scenarios are large enough for the solution methods via HS1 and HS2 to reach the optimal solution.
- 3) DBS (HS1) and RLS (HS2) have very similar performance on the best sample selection in IEEE-9, -57 and -118 systems, while DBS (HS1) outperforms RLS (HS2) on the worst sample selection in four systems. The main reason may be that DBS selects each sample based on the maximum average dissimilarity between the candidate sample and the previous all selected ones, while RLS selects samples by the maximum dissimilarity between the candidate sample and the most recently selected one.

Additionally, the runtimes (unit: second) of HS<sub>1</sub> and HS2 are provided Table VIII below in the runtime reduction is computed by (1-runtime(HS2)/runtime(HS1))\*100%. Though HS1 may

TABLE VIII
COMPARISON FOR RUNTIMES OF HS1 AND HS2

Case	HS1	HS2	Runtime Reduction
IEEE-5	0.66	0.28	57.57%
IEEE-9	0.74	0.38	48.65%
IEEE-57	5.58	3.41	38.89%
IEEE-118	42.75	13.12	69.31%



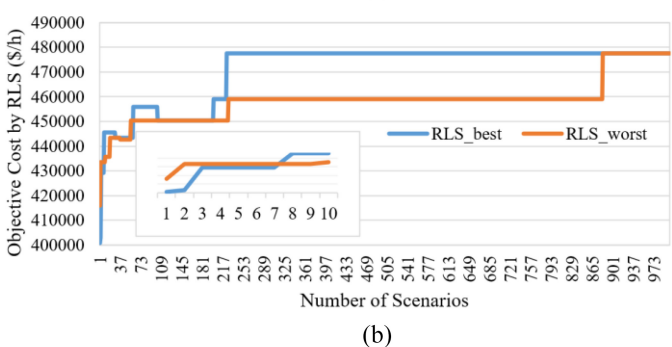


Fig. 7. (a) Performance of DBS in IEEE-5 System. (b) Performance of RLS in IEEE-5 System.

work better than HS2 on the sample selections from Table VI, HS2 is computationally more efficient than HS1 according to Table VIII. Specifically, using HS2, instead of HS1, will have about 40%-70% runtime reductions in these test systems. Hence, in the cases that requires considerable computational time, HS2 would be a promising alternative of HS1.

#### D. Verification of Learning-Based Sampling Methods

In the practical implementation of DBS or RLS, there is no need to repeat this verification process, but only *d* effective samples selected by DBS or RLS are used to solve the CC-PSO-ES problems. From a series of experimental simulations, in IEEE-5 system, *d* is suggested to be at least the number of the decision variables; IEEE-9, -57, and -118 systems can set *d* to be 10%-15% of the number of decision variables. The goal of this part is to trace how many effective samples selected by DBS or RLS are sufficient for achieving the objective costs in Table IV, i.e., to reveal the details of the sample selections in Table VI. Four sets of plots for verifying the effective samples selected by DBS and RLS in four IEEE test cases are displayed in Figs. 7–10 (a) and (b).

For the figures above, the x-axis denotes the number of scenarios used for solving the CC-PSO-ES problem with the

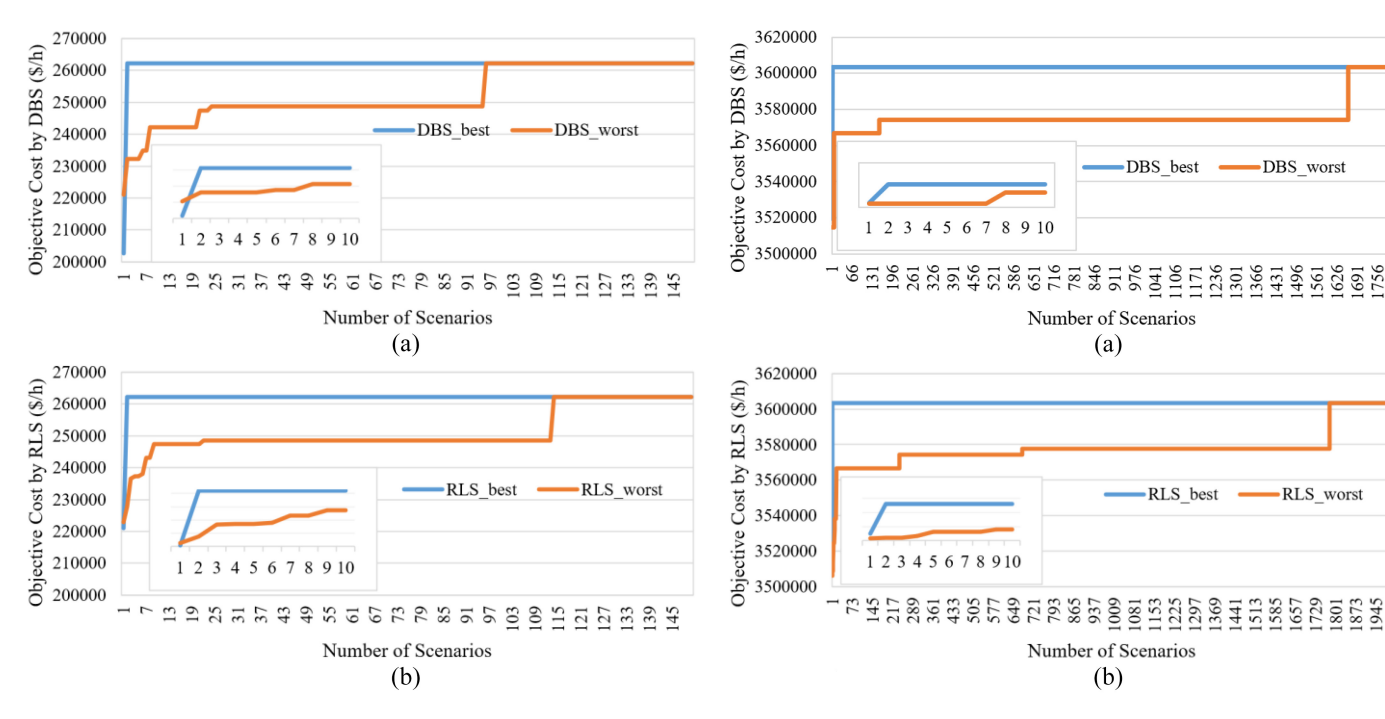
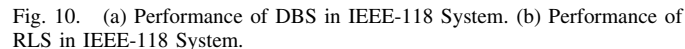


Fig. 8. (a) Performance of DBS in IEEE-9 System. (b) Performance of RLS in IEEE-9 System.



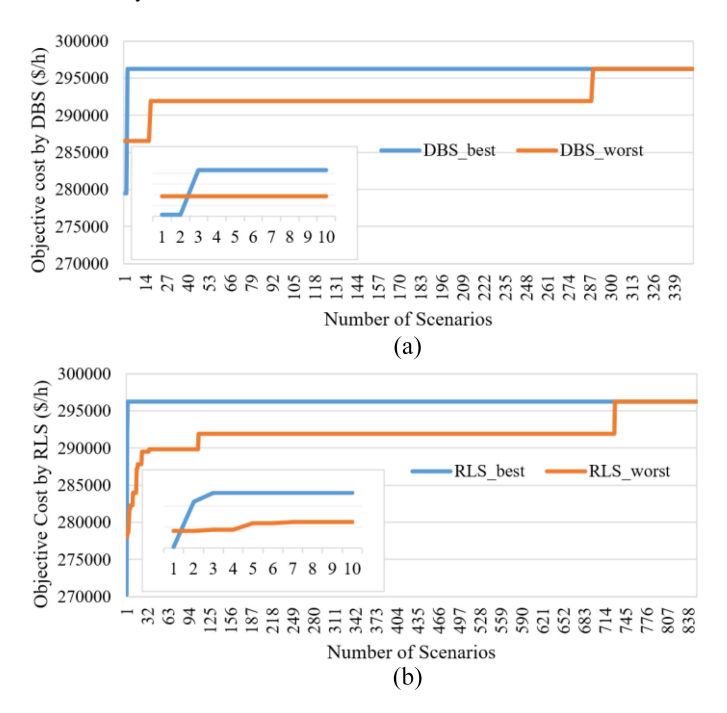


Fig. 9. (a) Performance of DBS in IEEE-57 System. (b) Performance of RLS in IEEE-57 System.

range of 1 to *N*, and the *y*-axis is the objective cost of the CC-PSO-ES problem. When the *x*-axis is more than the best (worst) sample size by DBS or RLS shown in Table VII, *y*-axis doesn't change in fact. Hence, the figures above ignore the results with *x*-axis more than the best (worst) sample size. To avoid the overlap of the results of DBS and RLS in the single figure, each set of figures has (a) and (b) figures, corresponding to using DBS and RLS, respectively. Each figure has a partial enlarged view at the left bottom

to reveal the result with x-axis from 1 to 10. There are two colored lines at each figure where DBS or RLS has blue and red lines corresponding to the best and worst selection results, denoted as 'DBS\_best' (blue) and 'DBS\_worst' (red), 'RLS best' (blue) and 'RLS worst' (red), respectively. Each pair of (a) and (b) figures are used to trace how the objective cost shown in Table V is achieved by the number of effective scenarios shown in Table VII. Once the sample sizes satisfy the values of Table VII, the optimal solutions (objective costs) are achieved and shown by the flattening lines. For instance, Fig. 7 (a), (b) show that the blue (red) line starts to be flatten when the sample size is more than 3 (432) using DBS, and 223 (883) using RLS, respectively, which is exactly in accord with the sample selection results of DBS and RLS from Table VII. In the same fashion, in IEEE-9, -57 and -118 systems, under the best sample selection results with 2~4 effective samples selected by DBS or RLS, the corresponding objective costs can be achieved and indicated by the flatten blue lines of partial enlarged views in Figs. 7-10. The red lines denote that the objective costs can be obtained with the worst selection results of DBS or RLS in Tables VII and shown at the top flat lines. Overall, the results of Figs. 7–10 are completely consistent with the sample selection results of DBS and RLS from Table VII.

Under different violation probabilities  $\epsilon=0.01\sim0.2$  and the confidence level fixed at 0.9999, the desired sample sizes required by the RSM used in [13], [15]–[18], FAST in [14], and the proposed method based on DBS are computed below in Tables IX–XI. Basically, three tables indicate that: 1) all sample sized decided by three methods will increase with the decrease in the violation probability, 2) the sample size by RSM is far more than the sample sizes by FAST and the proposed method, 3) the sample size by the proposed method

TABLE IX SAMPLE SIZE REQUIRED BY RSM

Case / €	0.01	0.025	0.075	0.1	0.2
IEEE-5	174643	69857	23286	17465	8733
IEEE-9	222643	89057	29686	22265	11133
IEEE-57	1182643	473057	157686	118265	59133
IEEE-118	3467443	1386977	462326	346745	173373

TABLE X
SAMPLE SIZE REQUIRED BY FAST

Case / €	0.01	0.025	0.075	0.1	0.2
IEEE-5	1787	1234	988	958	912
IEEE-9	2027	1474	1228	1198	1152
IEEE-57	6827	6274	6028	5998	5952
IEEE-118	18251	17698	17458	17422	17376

TABLE XI
SAMPLE SIZE REQUIRED BY THE PROPOSED METHOD

Case / $\epsilon$	0.01	0.025	0.075	0.1	0.2
IEEE-5	448	289	231	218	213
IEEE-9	219	135	95	94	88
IEEE-57	221	211	213	204	210
IEEE-118	1752	1675	1672	1671	1680

on average is much smaller than the sample size by FAST and bounded by the number of decision variables.

In practice, the decision-makers may be more interested in the solution with low violation probabilities. According to [13]–[18], the violation probability within 0.1 would give a satisfactory solution. Our experimental analysis shows that the objective costs on four cases have no significant changes with  $\epsilon=0.01\sim0.2$ , which is similar with the analysis in [17], [18] using the existing PD-free solution method for the CCO problems. The results in [17], [18] with changing the violation probabilities within 0.4 have little effect on the objective cost of the CCO problems. Specifically, the change in the objective cost with each ( $\pm0.05$ ) change in the violation probability is only 1% on average.

#### V. CONCLUSION AND FUTURE WORK

This paper presents a novel scenario-based solution method for solving the chance-constrained multi-period optimal power system operation (PSO) with battery energy storage (CC-PSO-ES), which is originally nonconvex and computationally intractable. The proposed method, which is based on the data-driven convex quadratic approximation (DDCQA) of ACPF and the strategic sampling, i.e., hybrid sampling methods, only uses a small number of scenarios without the pre-known PD of the uncertainty of PLREG, which is PD-free. The DDCQA is modified through the generalized LASSO and applied to address the nonconvex problem of ACPF

constraints in CC-PSO-ES problem. Unlike the RS-based methods, the hybrid sampling (HS) methods are proposed with dissimilarity-based learning and reinforcement learning methods. HS determines a smaller sample size than the RS-based methods. Eventually, the originally intractable CC-PSO-ES is converted to a tractable convex quadratic optimization problem with few effective scenarios. In our future work, we intend to test the proposed method in real-life large-scale power systems and further discuss the strategic sample selection from the aspects of using theoretical inference and advanced learning methods.

#### REFERENCES

- [1] Energy Storage Grand Challenge, 1st ed., U.S. Dept. Energy, Washington DC, USA, 2020, pp. 12–20.
- [2] M. Asensio and J. Contreras, "Stochastic unit commitment in isolated systems with renewable penetration under CVaR assessment," *IEEE Trans. Smart Grid*, vol. 7, no. 3, pp. 1356–1367, May 2016, doi: 10.1109/TSG.2015.2469134.
- [3] C. Zhao and Y. Guan, "Unified stochastic and robust unit commitment," IEEE Trans. Power Syst., vol. 28, no. 3, pp. 3353–3361, Aug. 2013, doi: 10.1109/TPWRS.2013.2251916.
- [4] F. Alismail, P. Xiong, and C. Singh, "Optimal wind farm allocation in multi-area power systems using distributionally robust optimization approach," *IEEE Trans. Power Syst.*, vol. 33, no. 1, pp. 536–544, Jan. 2018, doi: 10.1109/TPWRS.2017.2695002.
- [5] Z. Chen, D. Kuhn, and W. Wiesemann, "Data-driven chance constrained programs over wasserstein balls," 2018, arXiv:1809.00210.
- [6] H. Zhang and P. Li, "Chance constrained programming for optimal power flow under uncertainty," *IEEE Trans. Power Syst.*, vol. 26, no. 4, pp. 2417–2424, Nov. 2011, doi: 10.1109/TPWRS.2011.2154367.
- [7] A. Pena-Ordieres, D. K. Molzahn, L. A. Roald, and A. Waechter, "DC optimal power flow with joint chance constraints," *IEEE Trans. Power Syst.*, vol. 36, no. 1, pp. 147–158, Jan. 2021, doi: 10.1109/TPWRS.2020.3004023.
- [8] C. Ning and F. You, "Optimization under uncertainty in the era of big data and deep learning: When machine learning meets mathematical programming," Comput. Chem. Eng., vol. 125, pp. 434–448, Jun. 2019.
- [9] M. C. Campi and S. Garatti, "Wait-and-judge scenario optimization," Math. Program., vol. 167, no. 1, pp. 155–189, 2018.
- [10] G. Calafiore and M. C. Campi, "Uncertain convex programs: Randomized solutions and confidence levels," *Math. Program.*, vol. 102, no. 1, pp. 25–46, 2005.
- [11] A. Nemirovski and A. Shapiro, "Convex approximations of chance constrained programs," SIAM J. Optim., vol. 17, no. 4, pp. 969–996, 2007.
- [12] Q. Li, "Probability distribution-free general scenario programming," 2021, arXiv:2104.13494.
- [13] M. C. Campi and S. Garatti, "The exact feasibility of randomized solutions of uncertain convex programs," SIAM J. Optim., vol. 19, no. 3, pp. 1211–1230, 2008. [Online]. Available: https://doi.org/10.1137/ 07069821X
- [14] A. Carè, S. Garatti, and M. C. Campi, "FAST—Fast algorithm for the scenario technique," *Oper. Res.*, vol. 62, no. 3, pp. 662–671, Jun. 2014.
- [15] M. Vrakopoulou, B. Li, and J. L. Mathieu, "Chance constrained reserve scheduling using uncertain controllable loads part I: Formulation and scenario-based analysis," *IEEE Trans. Smart Grid*, vol. 10, no. 2, pp. 1608–1617, Mar. 2019, doi: 10.1109/TSG.2017.2773627.
- [16] B. Li, M. Vrakopoulou, and J. L. Mathieu, "Chance constrained reserve scheduling using uncertain controllable loads part II: analytical reformulation," *IEEE Trans. Smart Grid*, vol. 10, no. 2, pp. 1618–1625, Mar. 2019, doi: 10.1109/TSG.2017.2773603.
- [17] M. S. Modarresi et al., "Scenario-based economic dispatch with tunable risk levels in high-renewable power systems," *IEEE Trans.* Power Syst., vol. 34, no. 6, pp. 5103–5114, Nov. 2019, doi: 10.1109/TPWRS.2018.2874464.
- [18] H. Ming, L. Xie, M. C. Campi, S. Garatti, and P. R. Kumar, "Scenario-based economic dispatch with uncertain demand response," *IEEE Trans. Smart Grid*, vol. 10, no. 2, pp. 1858–1868, Mar. 2019, doi: 10.1109/TSG.2017.2778688.

- [19] J. Eason and S. Cremaschi, "Adaptive sequential sampling for surrogate model generation with artificial neural networks," *Comput. Chem. Eng.*, vol. 68, pp. 220–232, Sep. 2014.
- [20] X. Chen, "Exact computation of minimum sample size for estimation of binomial parameters," J. Stat. Plan. Inference, vol. 141, no. 8, pp. 2622– 2632, 2011.
- [21] T. Alamo, R. Tempo, and E. F. Camacho, "Randomized strategies for probabilistic solutions of uncertain feasibility and optimization problems," *IEEE Trans. Autom. Control*, vol. 54, no. 11, pp. 2545–2559, Nov. 2009, doi: 10.1109/TAC.2009.2031207.
- [22] R. Hu and Q. F. Li, "Efficient solution strategy for chance-constrained optimal power flow based on FAST and data-driven convexification," 2021, arXiv:2105.05336.
- [23] M. Aien, A. Hajebrahimi, and M. Fotuhi-Firuzabad, "A comprehensive review on uncertainty modeling techniques in power system studies," *Renew. Sustain. Energy Rev.*, vol. 57, no. 5, pp. 1077–1089, May 2016.
- [24] M. Yang, C. Shi, and H. Liu, "Day-ahead wind power forecasting based on the clustering of equivalent power curves," *Energy*, vol. 218, no. 5, 2021, Art. no. 119515.
- [25] R. Pless and R. Souvenir, "A survey of manifold learning for images," IPSJ Trans. Comput. Vis. Appl., vol. 1, pp. 83–94, Mar. 2009. [Online]. Available: https://doi.org/10.2197/ipsjtcva.1.83
- [26] Z. Xiang, Y. Bao, Z. Tang, and H. Li, "Deep reinforcement learning-based sampling method for structural reliability assessment," *Rel. Eng. Syst. Safety*, vol. 199, Jul. 2021, Art. no. 106901.
- [27] T. M. Moerland, J. Broekens, and C. M. Jonker, "Model-based reinforcement learning: A survey," 2020, arXiv:2006.16712.
- [28] M. A. Wiering and M. Van Otterlo, "Reinforcement learning," in Adaptation, Learning, and Optimization, vol. 12. Berlin, Germany: Springer, 2012.
- [29] T. Wang et al., "Benchmarking model-based reinforcement learning," 2019, arXiv:1907.02057.
- [30] S. M. Fatemi, S. Abedi, G. B. Gharehpetian, S. H. Hosseinian, and M. Abedi, "Introducing a novel DC power flow method with reactive power considerations," *IEEE Trans. Power Syst.*, vol. 30, no. 6, pp. 3012–3023, Nov. 2015.
- [31] R. Hu, Q. Li, and S. Lei, "Ensemble learning based linear power flow," in *Proc. IEEE Power Energy Soc. General Meeting (PESGM)*, Montreal, QC, Canada, 2020, pp. 1–5, doi: 10.1109/PESGM41954.2020.9281793.
- [32] R. A. Jabr, "Radial distribution load flow using conic programming," IEEE Trans. Power Syst., vol. 21, no. 3, pp. 1458–1459, Aug. 2006.
- [33] X. Bai, H. Wei, K. Fujisawa, and Y. Wang, "Semidefinite programming for optimal power flow problems," *Int. J. Elect. Power Energy Syst.*, vol. 30, nos. 6–7, pp. 383–392, 2008.
- [34] Q. Li, R. Ayyanar, and V. Vittal, "Convex optimization for DES planning and operation in radial distribution systems with high penetration of photovoltaic resources," *IEEE Trans. Sustain. Energy*, vol. 7, no. 3, pp. 985–995, Jul. 2016.
- [35] C. Coffrin, H. L. Hijazi, and P. Van Hentenryck, "The QC relaxation: A theoretical and computational study on optimal power flow," *IEEE Trans. Power Syst.*, vol. 31, no. 4, pp. 3008–3018, Jul. 2016.
- [36] D. K. Molzahn and I. A. Hiskens, "Sparsity-exploiting moment-based relaxations of the optimal power flow problem," *IEEE Trans. Power Syst.*, vol. 30, no. 6, pp. 3168–3180, Nov. 2015.
- [37] Q. Li and V. Vittal, "Convex hull of the quadratic branch AC power flow equations and its application in radial distribution networks," *IEEE Trans. Power Syst.*, vol. 33, no. 1, pp. 839–850, Jan. 2018.
- [38] Q. Li, "Uncertainty-aware three-phase optimal power flow based on data-driven convexification," *IEEE Trans. Power Syst.*, vol. 36, no. 2, pp. 1645–1648, Mar. 2021.
- [39] R. Hu, Q. Li, and F. Qiu, "Ensemble learning based convex approximation of three-phase power flow," *IEEE Trans. Power Syst.*, vol. 36, no. 5, pp. 4042–4051, Sep. 2021, doi: 10.1109/TPWRS.2021.3055481.
- [40] B. Kocuk, S. S. Dey, and X. A. Sun, "Inexactness of SDP relaxation and valid inequalities for optimal power flow," *IEEE Trans. Power Syst.*, vol. 31, no. 1, pp. 642–651, Jan. 2016.
- [41] Z. Y. Wang, D. S. Kirschen, and B. S. Zhang, "Accurate semidefinite programming models for optimal power flow in distribution systems," 2017, arXiv:1711.07853.
- [42] M. Gan, G.-Y. Chen, L. Chen, and C. L. P. Chen, "Term selection for a class of separable nonlinear models," *IEEE Trans. Neural Netw. Learn. Syst.*, vol. 31, no. 2, pp. 445–451, Feb. 2020, doi: 10.1109/TNNLS.2019.2904952.
- [43] V. Roth, "The generalized LASSO," *IEEE Trans. Neural Netw.*, vol. 15, no. 1, pp. 16–28, Jan. 2004, doi: 10.1109/TNN.2003.809398.

- [44] T. Hastie, R. Tibshirani, and R. Tibshirani, "Best subset, forward stepwise or Lasso? Analysis and recommendations based on extensive comparisons," *Stat. Sci.*, vol. 35, no. 4, pp. 579–592, 2020.
- comparisons," *Stat. Sci.*, vol. 35, no. 4, pp. 579–592, 2020. [45] R. J. Tibshirani and J. Taylor, "The solution path of the generalized Lasso," *Ann. Stat.*, vol. 39, no. 3, pp. 1335–1371, 2011.
- [46] D. Bienstock, M. Chertkov, and S. Harnett, "Chance-constrained optimal power flow: Risk-aware network control under uncertainty," *SIAM Rev.*, vol. 56, no. 3, pp. 461–495, 2014.
- [47] J. Hu and H. Li, "A new clustering approach for scenario reduction in multi-stochastic variable programming," *IEEE Trans. Power Syst.*, vol. 34, no. 5, pp. 3813–3825, Sep. 2019, doi: 10.1109/TPWRS.2019.2901545.
- [48] B. Li, K. Sedzro, X. Fang, B.-M. Hodge, and J. Zhang, "A clustering-based scenario generation framework for power market simulation with wind integration," *J. Renew. Sustain. Energy*, vol. 12, no. 3, 2020, Art. no. 036301.
- [49] A. Bellet, A. Habrard, and M. Sebban, "A survey on metric learning for feature vectors and structured data," 2013, arXiv:1306.6709.
- [50] P. Kundur, Power System Stability and Control. New York, NY, USA: McGraw-Hill Prof., 1994.
- [51] K. Purchala, L. Meeus, D. Van Dommelen, and R. Belmans, "Usefulness of DC power flow for active power flow analysis," in *Proc. IEEE Power Eng. Soc. General Meeting*, 2005, pp. 454–459.
- [52] C. Carleton and P. Van Hentenryck, "A linear-programming approximation of ac power flows," *INFORMS J. Comput.*, vol. 26, no. 4, pp. 718–734, 2014.
- [53] H. Hijazi, C. Coffrin, and P. Van Hentenryck, "Convex quadratic relaxations for mixed-integer nonlinear programs in power systems," *Math. Program. Comput.*, vol. 9, no. 3, pp. 321–367, 2017.
- [54] R. D. Zimmerman, C. E. Murillo-Sándnchez, and R. J. Thomas, "MATPOWER: Steady-state operations, planning, and analysis tools for power systems research and education," *IEEE Trans. Power Syst.*, vol. 26, no. 1, pp. 12–19, Feb. 2011.
- [55] R. D. Zimmerman, C. E. Murillo-Sanchez. (2020). MATPOWER (Version 7.1) [Software]. doi: 10.5281/zenodo.4074135.
- [56] M. E. Baran and F. F. Wu, "Optimal capacitor placement on radial distribution systems," *IEEE Trans. Power Del.*, vol. 4, no. 1, pp. 725–734, Jan. 1989, doi: 10.1109/61.19265.
- [57] D. Deka, S. Backhaus, and M. Chertkov, "Structure learning in power distribution networks," *IEEE Trans. Control Netw. Syst.*, vol. 5, no. 3, pp. 1061–1074, Sep. 2018.
- [58] P. Šulc, S. Backhaus, and M. Chertkov, "Optimal distributed control of reactive power via the alternating direction method of multipliers," *IEEE Trans. Energy Convers.*, vol. 29, no. 4, pp. 968–977, Dec. 2014, doi: 10.1109/TEC.2014.2363196.
- [59] "Energy, Load, and Demand Reports." ISO New England. 2020.
  [Online]. Available: https://www.iso-ne.com/isoexpress/web/reports/load-and-demand



Ren Hu (Graduate Student Member, IEEE) received the M.S. degree in electrical engineering from the South China University of Technology, Guangzhou, China, in 2013. He is currently pursuing the Ph.D. degree in electrical engineering with the University of Central Florida, Orlando, FL, USA. His research interests are machine learning and statistical inference applied in power and energy systems modeling, and optimization.



Qifeng Li (Senior Member, IEEE) received the Ph.D. degree in electrical engineering from Arizona State University, Tempe, AZ, USA, in 2016. He is currently an Assistant Professor with the Department of Electrical and Computer Engineering, University of Central Florida (UCF), Orlando, FL, USA. Before joining UCF Faculty, he held a position of a Postdoctoral Associate with the Department of Mechanical Engineering, Massachusetts Institute of Technology, Cambridge, MA, USA, from 2016 to 2018. His research interests include con-

vex optimization, uncertainty-aware optimization, and nonlinear systems with applications in power and energy systems.